Response to reviewer #1

We thank the reviewer for her/his in depth review comments that have help us to improve the clarity of the manuscript. Kindly find below our responses to each of the comments (quoted between []). We hope that our responses will address the main issues and that the changes made will convince that the IASI HNO$_3$ dataset has the potential to contribute to stratospheric studies and, more particularly, to the time evolution of the polar processes.

Major comments

[The major part of the data (2008-2016) reported in this manuscript was already published in Ronsmans et al. (2018), also together with temperatures at 50 hPa. For example, Fig. 4 (top) of the actual manuscript is a zoom of Fig. 3 of Ronsmans et al. (2018) to the southern latitudes with one Antarctic winter added.] This paper indeed builds on the study of Ronsmans et al. (2018) but it goes a step further in showing the potential of the IASI-HNO$_3$ dataset for polar stratospheric studies, which was not detailed in Ronsmans et al. (2018). If MLS allows resolving the HNO$_3$ profile between 11 km and 30 km, the potential of IASI lies in its exceptional spatial and temporal sampling. We demonstrate here that despite its limited vertical sensitivity forcing us to consider one total column, the information content that lies in the low-middle stratosphere is good enough to expand on polar stratospheric denitrification studies, usually performed using limb sounder measurements, and to continue their long-term record given the end of limb-observations in the microwave and thermal infrared spectral region.

[While Ronsmans et al. (2016) provide a first validation of the observations by comparison with FTIR solar absorption measurements, a characterization given the extreme conditions within the dark Antarctic polar vortex is missing. This is one of the majors concerns why I think the paper should not be published in ACP in its present form. However, it should be quite straightforward to provide at least a first comparison with HNO3 observations by the Microwave Limb Sounder (MLS) which has a large temporal and spatial overlap with the IASI dataset.] The referee is kindly invited to refer to the figure 3 (top and bottom panels) of Ronsmans et al. (2016) that presents the global distributions of the degrees of freedom for signal (DOFS, top panels) and of the altitude of maximum sensitivity of IASI to the HNO$_3$ profile, separately for January (left) and July (right) 2011, when the strong HNO$_3$ depletion occurs within the cold Antarctic winter. Figure 3 of Ronsmans et al. (2016) clearly shows DOFS of around 0.95-1.05 inside the Antarctic polar vortex, demonstrating the ability of IASI to measure a total column of HNO$_3$ even above these coldest regions. It is also worth to note here that the measurements characterized by a low vertical resolution (DOFS < 0.9) or a poor spectral fit have been filtered out of this analysis. This is now better mentioned in Section 2 of the revised manuscript:

"Quality flags similar to those developed for O$_3$ in previous IASI studies (Wespes et al., 2017) were applied a posteriori to exclude data (i) with a corresponding poor spectral fit (e.g. based on quality flags rejecting biased or sloped residuals, fits with maximum number of iteration exceeded), (ii) with less reliability (e.g. based on quality flags rejecting suspect averaging kernels, data with less sensitivity characterized by a DOFS lower than 0.9) or (iii) with cloud contamination (defined by a fractional cloud cover larger than 25 %)."

Despite the fact that a validation of the IASI measurements within the Antarctic polar vortex against ground-based FTIR measurements could not be provided (these observations requiring sunlight), we agree that an evaluation of the IASI measurements in the Antarctic night was missing. Hence, as

suggested by the referee, we have preformed cross-comparison with observations by MLS in three equivalent latitude bands (see Figure 1 here below). We would like to point out that we here compare total columns measured by IASI with VMR measured by MLS at several pressure levels that cover the highest sensitivity of IASI (at ~50 hPa, ~70 hPa and ~30 hPa for the sake of the comparison). Hence, the comparison of IASI columns with MLS measurements is mostly qualitative at this stage and differences are expected for this reason. Note also that we have preferred comparing IASI HNO_3 columns with VMR measured by MLS at specific levels instead of integrated columns calculated from MLS, given the difference in the sensitivity profile between IASI and MLS, the non-negligible IASI sensitivity to HNO_3 in the troposphere where MLS does not measure HNO_3 etc, which makes the integrated columns from IASI vs MLS not directly comparable. It should be pointed out finally that part of the differences between IASI and MLS are likely due to the different number of co-located data within the 2.5°x2.5° grid cells considered here for the comparison, with a much larger number of observations for IASI (through the quality filtering) than for MLS.

Despite this, the comparison shows similar spatial and seasonal variations between IASI total HNO_3 columns and MLS VMR between ~70 and 30 hPa in the different latitude bands, in particular, in the southernmost equivalent latitudes (see top panel). The strong HNO_3 depletion is well captured by both IASI and MLS measurements with a perfect match for the onset of the depletion. It further supports the good sensitivity of IASI to HNO_3 in the range of these pressure levels, justifying the methodology used in this study.

The cross-comparison with MLS is indeed insightful and gives further credit on the IASI observations during the polar night. That comparison figure between IASI and MLS has therefore been included in Section 2 of the revised manuscript and the text was changed to:
 "In order to expand on the comparisons against FTIR measurements which is impossible during the polar night, Figure 1 (top panel) presents the time series of daily IASI total HNO_3 columns co-located with MLS VMR measurements within 2.5x2.5 grid boxes at three pressure levels (at 30, 50 and 70 hPa), averaged in the 70°S–90°S equivalent latitude band. Similar variations in HNO_3 are captured by the two instruments with an excellent agreement for the timing of the strong HNO_3 depletion within the inner vortex core. IASI HNO_3 variations generally match well those of MLS HNO_3 in each latitude band (see Figure 1 bottom panel for the 50°S–70°S equivalent latitude band; the other bands are not shown here)."

Specific comments

[L3, 'good vertical sensitivity': This has not been shown in this paper. It is necessary to demonstrate this for the dataset discussed here given the cold Antarctic stratosphere.]
As stated in the text, we here refer to "a good vertical sensitivity in the low and middle stratosphere", not to a good vertical resolution of the measurement.

As mentioned in the manuscript, this paper builds on the previous studies of Ronsmans et al. (2016) and (2018). Despite a poor vertical resolution between the retrieved layers forcing us to consider a total column, the sensitivity of IASI to HNO_3 was shown to vary with altitude and to be highest in the low-middle stratosphere, even within the cold Antarctic polar vortex (Ronsmans et al. (2016)). This means that the variability in the measured total column is mainly representative of that layer. As said above, we recall here that similarly to the earlier studies, HNO_3 measurements characterized by a poor spectral fit or by a low vertical sensitivity (DOFS < 0.9) have been filtered out of this analysis. This is now clearly mentioned in Section 2 of the revised manuscript:

"Quality flags similar to those developed for O_3 in previous IASI studies (Wespes et al., 2017) were applied a posteriori to exclude data (i) with a corresponding poor spectral fit (e.g. based on quality flags rejecting biased or sloped residuals, fits with maximum number of iteration exceeded), (ii) with less reliability (e.g. based on quality flags rejecting suspect averaging kernels, data with less sensitivity characterized by a DOFS lower than 0.9) or (iii) with cloud contamination (defined by a fractional cloud cover larger than 25 %)."

[L8, 'denitrification': Are you certain, that 'denitrification' is also used for the uptake of HNO3 in particles? Perhaps 'removal from the gas phase'.]
We thank the referee for this remark. We are of course aware that the so-called "denitrification" defines the permanent removal of NOy from an airmass due to the gravitational sedimentation of NOy-containing particles. We agree that, from IASI, we can only measure a "removal from the gas phase", caused by sequestration into particles with or without sedimentation. Careful attention has now been made in the manuscript to avoid abusive use of the term "denitrification". Hence, "onset of HNO_3 denitrification" has been changed to "the onset of HNO_3 depletion" where appropriated in the revised manuscript. The title has also been changed accordingly to:
"Polar stratospheric HNO_3 depletion surveyed from a decadal dataset of IASI total columns".

[L59, 'a maximum sensitivity in the mid-stratosphere around 50 hPa': This must be shown here for the extreme conditions in the Antarctic vortex - also since all later analyses in the paper use temperatures at 50 hPa. What is the vertical variability of this level of maximum sensitivity within the development inside the vortex, especially later in the winter when, due to sedimentation of PSC particles, HNO3 concentrations at those levels are very low?]
See our responses to the general comments. Here again, we refer to the figure 3 (top and bottom panels) of Ronsmans et al. (2016) that presents the global distributions of the degrees of freedom for signal (DOFS, top panels) and of the altitude of maximum sensitivity of IASI to the HNO_3 profile (bottom panel), separately for January (left) and July (right) 2011, when the strong HNO_3 depletion occurs within the cold Antarctic winter. It shows clearly that the altitude of maximum sensitivity of the total columns is invariant at equatorial and tropical latitudes, whereas it varies with seasons at middle and polar latitudes. Above the Antarctic, the altitude of maximum sensitivity varies between ~9 km in summer and ~22 km in winter. The variations of the altitude of maximum sensitivity follow the altitude variations of maximum HNO_3 concentrations.

This is now more explicit at several places in the revised manuscript; e.g. in Section 1: "IASI provides reliable total column measurements of HNO_3 characterized by a maximum sensitivity in the low-middle stratosphere around 50 hPa (20 km) during the dark Antarctic winter (Ronsmans et al., 2016; 2018) …" and in Section 2: "… the largest sensitivity of IASI in the region of interest, i.e. in the low and mid-stratosphere (from 70 to 30 hPa), where the HNO_3 abundance is the highest (Ronsmans et al., 2016).

In order to convince the referee that IASI measurements capture the expected variations of HNO_3 within the polar night, we provide in Figure 2 below examples of vertical HNO_3 profiles retrieved within the dark Antarctic vortex (above Arrival Height) and outside the vortex (above Lauder). The retrieved profiles are shown along with their associated total retrieval error and averaging kernels (the total column AvK and the so-called "sensitivity profile" are also represented). The sum of the averaging kernels indicates how the true state at a specific altitude changes the retrieved total column, i.e. the altitude to which the retrieved total column is mainly sensitive/representative. Above Arrival Height during the dark Antarctic winter, we clearly see depleted HNO_3 levels in the low and mid-stratosphere and the altitude of maximum sensitivity at around 30 hPa. At Lauder on the contrary, HNO_3 levels larger than the a priori are observed in the stratosphere with a larger range of maximum sensitivity.

3

[L79, 'The total columns yield a total retrieval error of 10% and a low bias (10.5%) compared to ground-based FTIR measurements (Hurtmans et al., 2012; Ronsmans et al., 2016).': As these numbers are used also later in the manuscript, their validity has to be confirmed for the condition in the dark vortex, which cannot be achieved with comparisons to sun-dependent FTIR observations. As mentioned above, I strongly suggest to perform comparisons with the MLS dataset.]

Figure 4 of Ronsmans et al. (2016) illustrates the global distribution of the total retrieval error for HNO_3 (integrated over 5 to 35 km) separately for January (left) and July (right) over the period of the IASI measurements. The mid- and polar latitudes are characterized by low total retrieval errors of around ~3-5% - which corresponds to a reduction by a factor of 18-30 compared to the prior uncertainty (90%) and indicates a real gain of information – except above Antarctica during wintertime where the errors reach 25%. They are explained by (1) a weaker sensitivity (i.e. a larger smoothing error which represents in all cases the larger source of the retrieval error) above such cold surface (DOFS of ~0.95 within the dark Antarctic vortex – see figure 3 of Ronsmans et al., 2016) and by (2) a misrepresentation of the wavenumber-dependent surface emissivity above ice surface (Hurtmans et al., 2012). This is made more explicit in Section 2 of the revised manuscript:

"The total columns are associated with a total retrieval error ranging from around 3% at mid- and polar latitudes to 25% above cold Antarctic surface during winter (due to a weaker sensitivity above very cold surface with a DOFS of ~0.95 and to an poor knowledge of the seasonally and wavenumber-dependent emissivity above ice surfaces which induces larger forward model errors), and a low bias (lower than 12%) in polar regions over the altitude range where the IASI sensitivity is largest, when compared to ground-based FTIR measurements (see Hurtmans et al., 2012; Ronsmans et al., 2016 for more details)."

A validation against ground-based sun-dependent FTIR measurements could not be provided during the dark Antarctic winter, we refer on the good agreement with MLS (suggested by the referee) to underline the potentiality of IASI to detect the HNO_3 variations as well within the Antarctic winter (see general comment).

[L105, 'These high HNO_3 levels result from low sunlight…': This is not the only, and probably not the central explanation for the increasing column amounts. Dynamical effects on total columns of stratospheric gases (downwelling within the vortex) have to be considered.]

We thank the referee for this correction. The sentence has been rewritten as follows:

"These high HNO_3 levels result from low sunlight, preventing photodissociation, along with the heterogeneous hydrolysis of N_2O_5 to HNO_3 during autumn before the formation of polar stratospheric clouds (Keys et al., 1993; Santee et al., 1999; Urban et al., 2009; DeZafra et al., 2001). This period also corresponds to the onset of the deployment of the southern polar vortex which is characterized by strong diabatic descent with weak latitudinal mixing across its boundary, isolating polar HNO_3-rich air from lower latitudinal airmasses."

[Figure 2: I think the vertical dashed line '10Jun09' does not fit to the minimum of the solid blue curve (?)]

The referee is right; there was a bug for the automatically detection of the drop temperature, as well as for the detection of the corresponding dates in this figure. The figure has been corrected. The position of the drop temperatures does now perfectly match the yearly minima of the total HNO_3 second derivative. An average drop temperature over the ten years of IASI of 194.2 +/- 3.8 K is now calculated, which is even closer to T_{NAT}.

[L154, 'in the areas of potential vorticity smaller than -10 …': PV at which potential temperature level is used here?]

As mentioned in Section 2 of the submitted manuscript, "the potential vorticity (PV) fields are taken from the ECMWF ERA Interim Reanalysis dataset at the potential temperature of 530 K (corresponding to ~20 km altitude where the IASI sensitivity to HNO_3 is the highest during the Southern Hemisphere (S.H.) winter (Ronsmans et al., 2016)".

[L159, 'Note that the HNO_3 time series has been smoothed': As the drop temperatures (and dates) are introduced as the central new method presented in the manuscript, it is necessary to explore their behaviour in more detail. Can you give an estimate of the error of this measure by considering e.g. the effect of the numerical smoothing. Please show also the 1st derivative to be able to judge on the uncertainties of the 2nd derivative. How do the drop temperatures vary when using different pressure levels (e.g. 70 hPa)?]

As explained in the text, we actually only used a simple robust spline smoothing function to fill gaps in the time series, hence it has no particular impact on the detection of the drop temperature and its corresponding date.

Figure 3 here below represents the figure 2 of the manuscript along with the 1st derivative of HNO_3 total column with respect to time superimposed, as asked by the referee. We can clearly see that the minima of the 2nd derivative match or just precede those of the 1st derivative of total HNO_3 with respect to time.

Figure 4 below represents the figure 2 of the manuscript but for the temperature at 30 hPa (top panel) and 70 hPa (bottom panel) for the sake of comparison. As expected, the drop temperatures are the lowest when using the temperatures at 30 hPa. They vary from 185-195 K (~192K on average) at 30 hPa to 195-204 K (~198 K on average) at 70 hPa with values of ~189-202 K (~194 K on average) at 50 hPa.

As explained in the manuscript, the use of the 195 K at 50 hPa as single level for the analysis is justified by the fact that it corresponds best to the maximum of IASI vertical sensitivity during the polar night (see Figure 3 of Ronsmans et al. 2016 and responses to related comments above); another justification is found a posteriori by the consistency between the 195 K threshold temperature taken at 50 hPa and the onset of the strong total HNO_3 depletion seen by IASI, which matches the NAT development that occurs in June around that level. However, we fully agree that the HNO_3 abundances over a large part of the stratosphere (between 70 and 30 hPa) contribute to the total HNO_3 variations detected by IASI and that this inevitably affects the drop temperature calculation at 50 hPa. In order to address this issue, we have added in the manuscript the range of drop temperatures when calculated at these two other pressure levels (from 185 K to 204 K); this indeed allows the reader to better judge on the uncertainty of the drop temperature at 50 hPa (189-202 K). We thank the referee for his suggestion. The text in the revised manuscript is changed to:

"… Nevertheless, given the range of maximum IASI sensitivity to HNO_3 around 50 hPa, typically between 70 and 30 hPa (Ronsmans et al., 2016), the drop temperatures are also calculated at these two other pressure levels (not shown here) to estimate the uncertainty of the calculated drop temperature defined in this study at 50 hPa. The 30 hPa and 70 hPa drop temperatures range respectively over 185.7 K – 194.9 K and over 194.8 K – 203.7 K, with an average of 192.0 +/- 2.9 K and 198.0 +/- 3.2 K (1σ standard deviation) over the ten years of IASI. The average values at 30 hPa and 70 hPa fall within the 1σ standard deviation associated with the average drop temperature at 50 hPa. It is also worth noting the agreement between the drop temperatures and the NAT formation threshold at these two pressure levels (T_{NAT} ~193 K at 30 hPa and ~197 K at 70 hPa) (Lambert et al., 2016)."

[L184, 'The calculated drop temperatures vary significantly between 180 and 210 K. These high extremes are only found in very few cases and should be considered with caution as they correspond to specific regions above ice shelves with emissivity features that are known to yield errors in the IASI retrievals': I find the discussion around the deviations of the drop temperatures very confusing. At the beginning of the manuscript it is stated, that the error of the measured total column amounts is in the order of 10%. Here it is argued that 'above ice shelves' it might be higher. Also, in Fig. 5 one can see that there are large regions over eastern Antarctica where drop temperatures are often clearly above 195K even inside the red circles. This is not explained satisfactorily in the manuscript. Here, again, it would be important to investigate on the reliability, consistency and homogeneity of the IASI HNO3 values. As mentioned above, this could be accomplished with a comparison to MLS observations.]

See our response above about the characterization of the HNO_3 retrievals in terms of total retrieval error and of its spatial/temporal distribution: The largest errors (25%) are found above Antarctica during wintertime and are due to (1) a weaker sensitivity (i.e. a larger smoothing error which represents in all cases the larger source of the retrieval error) above such cold land surface (DOFS of ~0.95 within the dark Antarctic vortex – see figure 3 of Ronsmans et al., 2016) and to (2) a poor knowledge of the (seasonally and wavenumber-dependent) emissivity of ice surfaces (Hurtmans et al., 2012). This is now clearly mentioned in Section 2 of the revised manuscript.

Bright land surface such as desert or ice might in some cases lead to poor HNO_3 retrievals due to a poor knowledge of the wavenumber-dependent emissivity above such surfaces, which can alter the retrieval by compensation effects (Wespes et al., 2009). FORLI relies on the monthly climatology of surface emissivity built by Zhou et al. (2011) from several years of IASI measurements on a 0.5x0.5 grid and for each 8461 IASI spectral channels when available, or on the MODIS climatology that is unfortunately restricted to only 12 channels in the IASI spectral range; see Hurtmans et al. (2012) for more details. Although wavenumber-dependent surface emissivity atlases are used in FORLI, it is clear that this parameter remains critical and causes poorer retrievals that, in some instances, pass the posterior filtering. The total HNO_3 columns over eastern Antarctica which show drop temperatures much above 195K might precisely be related to this. We have made this clear in Section 4.2 of the revised version:

"…emissivity features that are known to yield errors in the IASI retrievals. Indeed, bright land surface such as ice might in some cases lead to poor HNO_3 retrievals. Although wavenumber-dependent surface emissivity atlases are used in FORLI (Hurtmans et al., 2012), this parameter remains critical and causes poorer retrievals that, in some instances, pass through the series of quality filters and affect the drop temperature calculation."

[L195, 'Overall, despite these limitations, the spatial variability in the drop 50 hPa temperatures for IASI total HNO_3 is well in agreement with the natural variation in PSCs nucleation temperatures': Given the extended areas where the drop temperatures are larger than 195K, this statement is not convincing.]

The sentence has been rewritten for clarity:

"Except above some parts of Antarctica which are prone to larger errors, the overall range in the drop 50 hPa temperature for total HNO_3, inside the isocontour for the 195 K temperature, typically extends from ~187 K to 195 K, which fall within the range of PSCs nucleation temperature at 50 hPa …".

Furthermore, in response to G. Manney and M. Santee, the contour of $-10 \times 10^{-5} K.m^2.kg^{-1}.s^{-1}$ based on the minimum PV encountered at 50 hPa over the 10 May to 15 July period as well as the isocontours of 195 K at 50 hPa for the averaged temperatures and the minima over the same period are also now represented in the revised Fig.5 and the distribution of the drop temperatures is much better described and explained in the revised version:

6

"The averaged isocontour of 195 K encircles well the area of HNO_3 drop temperatures lower than 195 K, which means that the bins inside that area characterize airmasses that experience the NAT threshold temperature during a long time over the 10 May – 15 July period. That area encompasses the inner vortex core (delimited by the isocontour of $-10\times10^{-5}K.m^2.kg^{-1}.s^{-1}$ for the averaged PV), but is larger, and show pronounced minima (lower than $-0.5\ x10^{14}$ molec.cm^{-2}.d^{-2}) in the second derivative of the HNO_3 total column with respect to time (not shown here), which indicate a strong and rapid HNO_3 depletion.

The area enclosed between the two isocontours of 195 K for the temperatures, the averaged one and the one for the minimum temperatures, show higher drop temperatures and weakest minima (larger than $-0.5\ x10^{14}$ molec.cm^{-2}.d^{-2}) in the second derivative of the HNO_3 total column (not shown). That area is also enclosed by the isocontour of $-10\times10^{-5}K.m^2.kg^{-1}.s^{-1}$ for the minimum PV, meaning that the bins inside correspond, at least for one day over the 10 May – 15 July period, to airmasses located at the inner edge of the vortex and characterized by temperature lower than the NAT threshold temperature. The weakest minima in the second derivative of total HNO_3 (not shown) observed in that area indicate a weak and slow HNO_3 depletion and might be explained by a short period of the NAT threshold temperature experienced at the inner edge of the vortex. It could also reflect a mixing with strong HNO_3-depleted and colder airmasses from the inner vortex core. The mixing with these "already" depleted airmasses could also explained the higher drop temperatures detected in those bins. Finally, note also that these high drop temperatures are generally detected later (after the HNO_3 depletion occurs, i.e. after the 10 May – 15 July period considered here – not shown), which supports the transport, in those bins, of earlier HNO_3-depleted airmasses and the likely mixing at the edge of the vortex."

[L204, 'denitrification phase': See statement about 'denitrification' above.]
See our response above.

[L230, 'To the best of our knowledge, it is the first time that such a large satellite observational data set of stratospheric HNO3 concentrations is exploited to monitor the evolution HNO3 versus temperatures.': This sounds somehow exaggerated given all the previous work on HNO3/temperature/PSCs, e.g. by use of the MLS dataset and also since the correlation with temperature has already been shown in Ronsmans et al., 2018.]
We here simply refer to the unprecedented potential of IASI in terms of its exceptional spatial and temporal sampling. Ronsmans et al. (2018) also referred to the IASI dataset and correlations with temperature were done but in a lesser extent. In order to avoid overselling, the sentence has been rewritten:
"We show in this study that the IASI dataset allows capturing the variability of stratospheric HNO_3 throughout the year (including the polar night) in the Antarctic. In that respect, it offers a new observational means to monitor the relation of HNO_3 to temperature and the related formation of PSCs."

Technical comments:

L27, '(e.g. (Toon…))': I think the inner bracket level is not necessary.
L30, 'sedimentation(Lambert …): Space missing
L34, 'temperature': 'temperatures'
L51: Bracket levels?
L102, 'The red vertical line in Fig. 1a and Fig. 1b': There is no vertical red line in Fig. 1a. You mean horizontal?
L106, references: Brackets seem wrong.
Figure 2, caption, 'in the70—': Space missing.
L155, 'and the total HNO3 depletion are the coldest': Makes no sense.

L164, 'temperature are': 'temperatures are'
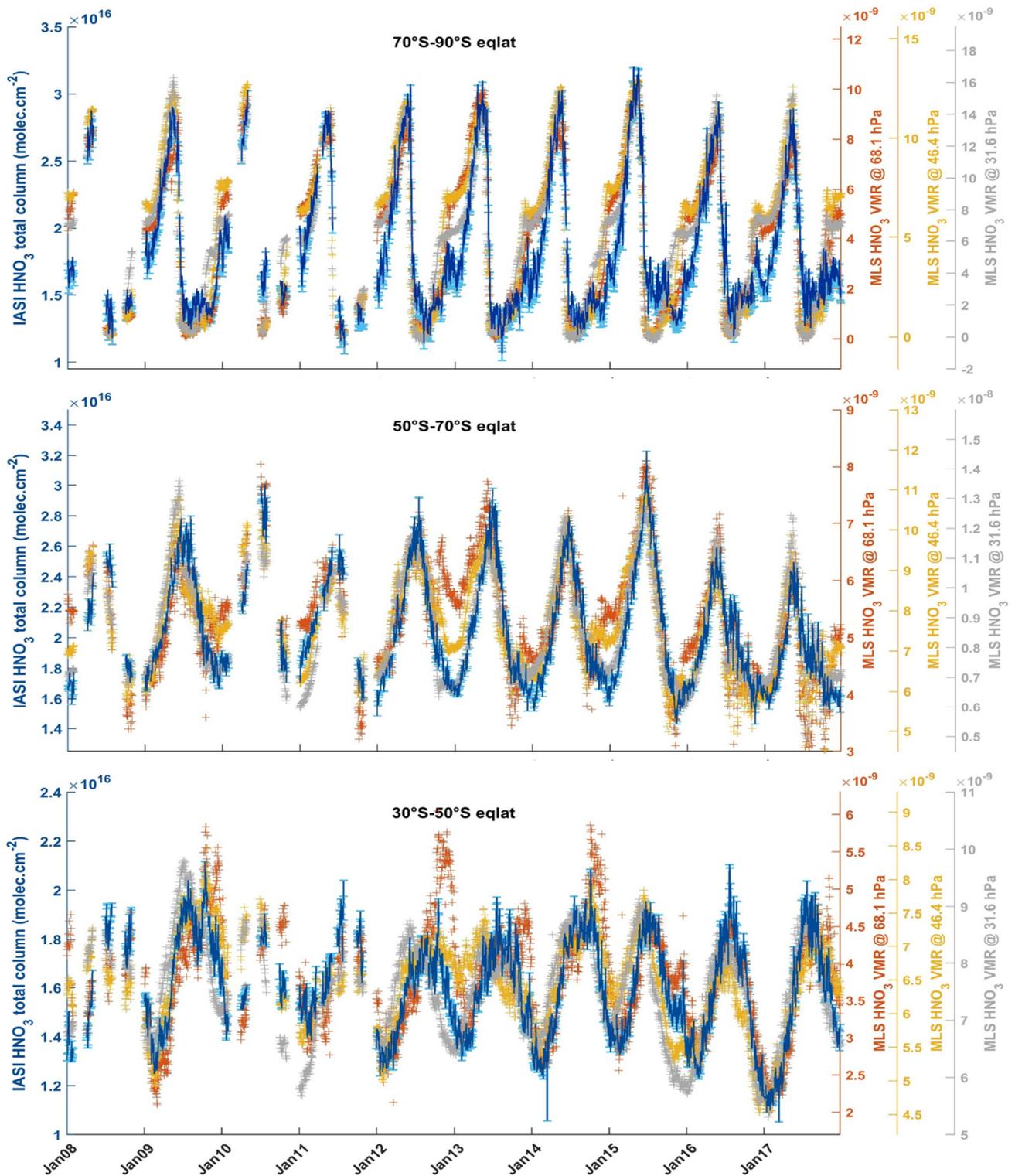
All the technical comments have been corrected.

Figure 1. Time series of daily IASI total HNO$_3$ column (blue, left y-axis) co-located with MLS and of MLS VMR HNO$_3$ within 2.5x2.5 grid boxes at three pressure levels (at 30, 50 and 70 hPa; right y-axis), averaged in the 70°S–90°S (top panel), the 50°S–70°S (middle panel) and in the 30°S–50°S (bottom panel) equivalent latitude bands. The error bars (light blue) represents 3σ, where σ is the standard deviation around the IASI HNO$_3$ daily average.
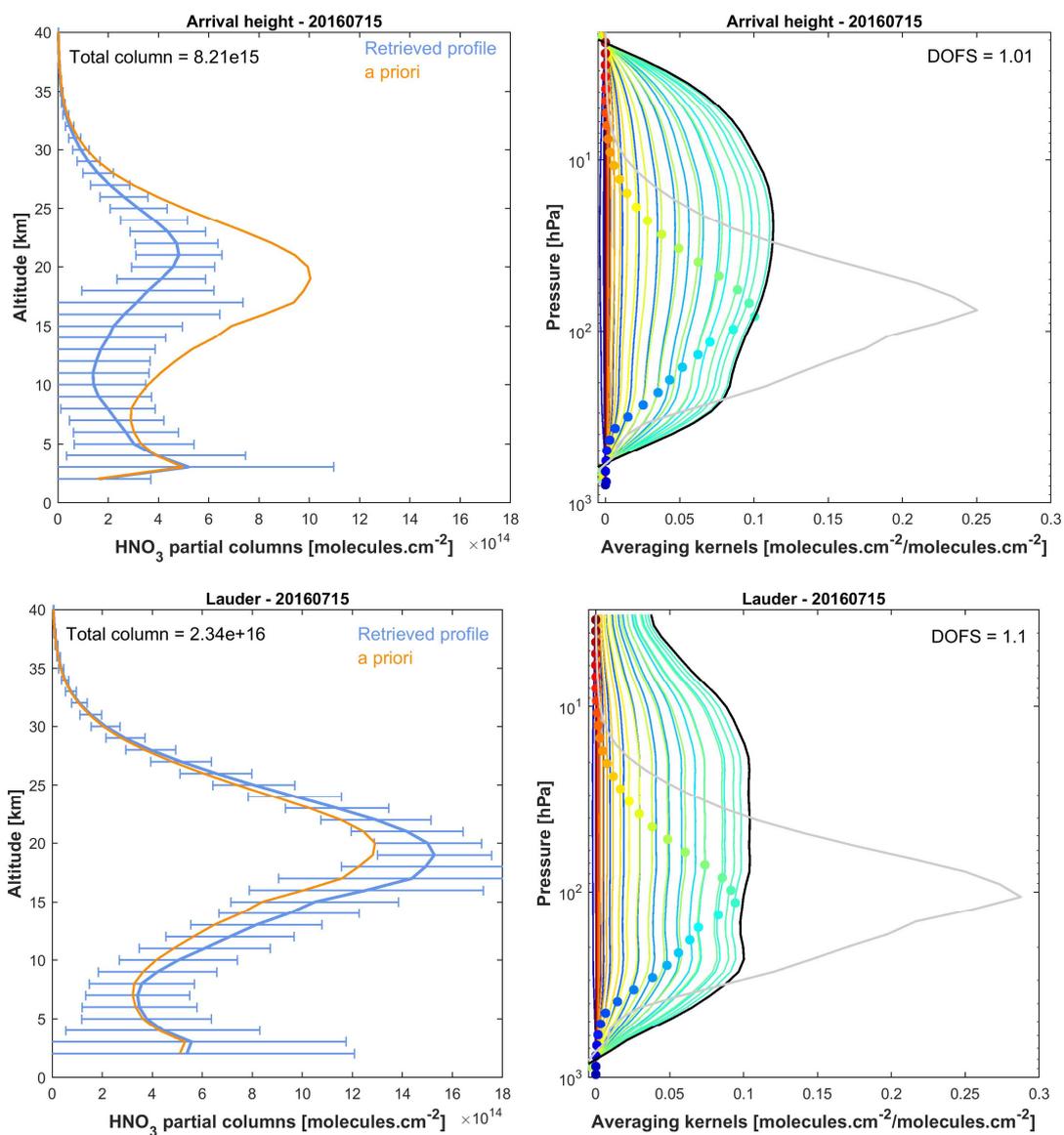
9

Figure 2. Examples of IASI HNO_3 vertical profiles (in molec.cm^{-2}) with corresponding averaging kernels (in molec.cm^{-2}/molec.cm^{-2}; with the total column averaging kernels (black) and the sensitivity profiles (grey)) above Arrival Height (77.49°S, 166.39°E, top panels) and Lauder (45.03°S, 169,40°E; bottom panels). The error bars associated with the HNO_3 vertical profile represent the total retrieval error. The a priori profile is also represented. The total column and the DOFS values are indicated.
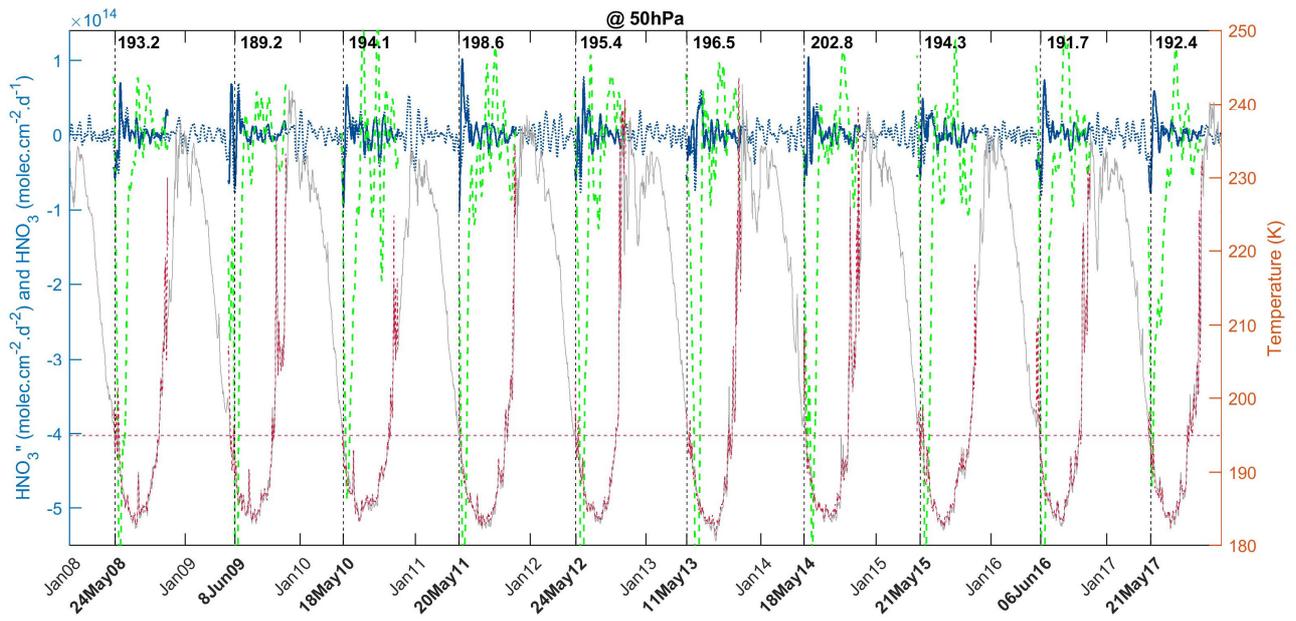
Figure 3. Time series of total HNO$_3$ first derivative (green, left y-axis), of total HNO$_3$ second derivative (blue, left y-axis) and of the temperature at 50 hPa (red, right y-axis), in the region of potential vorticity lower than -10 x10^{-5} K.m^2.kg^{-1}.s^{-1}. The red horizontal line corresponds to the 195 K temperature. The vertical dashed lines indicate the second derivative minimum in HNO$_3$ for each year. The corresponding dates (in bold, on the x-axis) and temperatures are also indicated. The time series of total HNO$_3$ second derivative (dashed blue) and of temperature at 50 hPa (grey) in the 70–90°S Eqlat band are also represented.
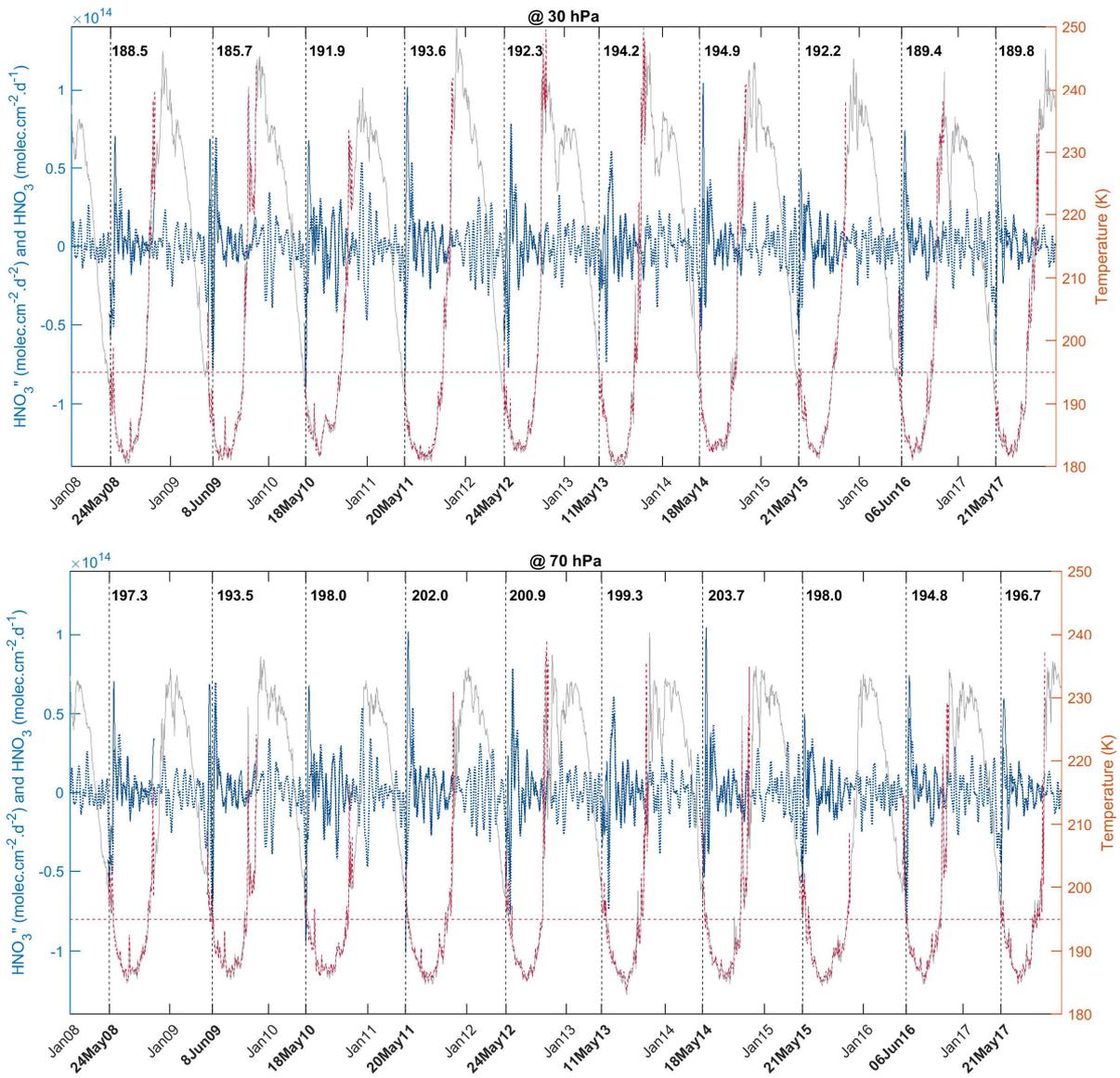
Figure 4. Same as Figure 3 but for the temperature at 30 hPa (top panel) and 70 hPa (bottom panel).